

Observation of piezoelectricity in free-standing monolayer MoS₂

Hanyu Zhu^{1†}, Yuan Wang^{1†}, Jun Xiao¹, Ming Liu¹, Shaomin Xiong¹, Zi Jing Wong¹, Ziliang Ye¹, Yu Ye¹, Xiaobo Yin^{1,2} and Xiang Zhang^{1,2*}

Piezoelectricity allows precise and robust conversion between electricity and mechanical force, and arises from the broken inversion symmetry in the atomic structure^{1–3}. Reducing the dimensionality of bulk materials has been suggested to enhance piezoelectricity⁴. However, when the thickness of a material approaches a single molecular layer, the large surface energy can cause piezoelectric structures to be thermodynamically unstable⁵. Transition-metal dichalcogenides can retain their atomic structures down to the single-layer limit without lattice reconstruction, even under ambient conditions⁶. Recent calculations have predicted the existence of piezoelectricity in these two-dimensional crystals due to their broken inversion symmetry⁷. Here, we report experimental evidence of piezoelectricity in a free-standing single layer of molybdenum disulphide (MoS₂) and a measured piezoelectric coefficient of $e_{11} = 2.9 \times 10^{-10} \text{ C m}^{-1}$. The measurement of the intrinsic piezoelectricity in such free-standing crystals is free from substrate effects such as doping and parasitic charges. We observed a finite and zero piezoelectric response in MoS₂ in odd and even number of layers, respectively, in sharp contrast to bulk piezoelectric materials. This oscillation is due to the breaking and recovery of the inversion symmetry of the two-dimensional crystal. Through the angular dependence of electromechanical coupling, we determined the two-dimensional crystal orientation. The piezoelectricity discovered in this single molecular membrane promises new applications in low-power logic switches for computing and ultrasensitive biological sensors scaled down to a single atomic unit cell^{8,9}.

Since its discovery in 1880, piezoelectricity has found a wide range of applications in actuation, sensing and energy harvesting. The rapidly growing demand for high-performance and miniaturized devices in micro-electro-mechanical systems (MEMS) and electronics^{10–12} calls for nanoscale piezoelectric materials, motivating theoretical investigations into novel low-dimensional systems such as nanotubes and single molecules^{13,14}. Transition-metal dichalcogenides (TMDCs) are ideal candidates as low-dimensional piezoelectric materials because of their structural non-centrosymmetry⁷. Although there has been extensive research interest in the unique properties originating from such symmetry breaking, including circular dichroism and second harmonic generation (SHG)^{15–19}, experimental quantitative determination of the intrinsic piezoelectric properties of these two-dimensional crystals has yet to be demonstrated. Here, we report the observation of piezoelectricity in free-standing monolayer MoS₂ membranes. Interestingly, we found that this molecular piezoelectricity only exists when there are an odd number of layers in the two-dimensional crystal where

inversion symmetry breaking occurs. We observed an angular dependence of the piezoelectric response in agreement with the three-fold symmetry of the crystal, and based on this we developed an effective method to determine the absolute two-dimensional crystal orientation.

The single piezoelectric coefficient e_{11} can fully describe the anisotropic electromechanical coupling in monolayer MoS₂ due to its crystalline D_{3h} symmetry (Fig. 1). The membrane has one atomic layer of Mo between two identical S layers, packed in a hexagonal lattice. Each rhombic prismatic unit cell is asymmetrically occupied by two S atoms on the left site and one Mo atom on the right, such that an external electric field pointing from the S site to the Mo site in the hexagonal lattice (armchair direction, E_1) can deform the unit cell by stretching the Mo–S bond and cause internal piezoelectric stress (Fig. 1b). Further analysis based on the three-fold rotational symmetry shows the induced piezoelectric stress tensor has only one independent component, $\Delta\sigma_p = \Delta\sigma_{11} = -\Delta\sigma_{22}$, which is proportional to the electric field²⁰:

$$\Delta\sigma_p = -e_{11}E_1 \quad (1)$$

To observe piezoelectricity, the conventional method is to measure the dipole induced by strain, as carried out in nanowires²¹ and very recently in supported MoS₂ on polymer substrates²². However, the interaction between the two-dimensional crystal and the substrate in such flexible devices makes quantitative determination of the intrinsic piezoelectric properties challenging. The other commonly used technique, piezoresponse force microscopy (PFM), measures picometre deformations with nanometre spatial resolution²³, and allows the quantitative determination of the piezoelectric constant²⁴. Unlike in conventional PFM, the MoS₂ membrane is not coupled to the vertical electric field between the tip and substrate due to its mirror symmetry along the z -axis. We have therefore developed a method that combines a laterally applied electric field²⁵ and nano-indentation²⁶ in an atomic force microscope (AFM) to measure the piezoelectrically generated membrane stress (Fig. 1c). A free-standing MoS₂ stripe was used to avoid substrate effects such as doping and parasitic charges, so as to accurately determine the intrinsic piezoelectricity. First, to convert the in-plane stress to an out-of-plane force, the free-standing film was indented by an AFM probe and deformed. Piezoelectric stress was then induced by an in-plane electric field applied through the lateral electrodes. The extra field-induced stress changed the load on the tip and the curvature of the cantilever, which was measured via the reflection of a laser beam from the cantilever. We could then quantify the piezoelectric responses of the monolayer MoS₂ crystal (equation (1)).

¹NSF Nano-scale Science and Engineering Center (NSEC), University of California at Berkeley, 3112 Etcheverry Hall, Berkeley, California 94720, USA.

²Material Sciences Division, Lawrence Berkeley National Laboratory, 1 Cyclotron Road, Berkeley, California 94720, USA. [†]These authors contributed equally to this work. *e-mail: xiang@berkeley.edu

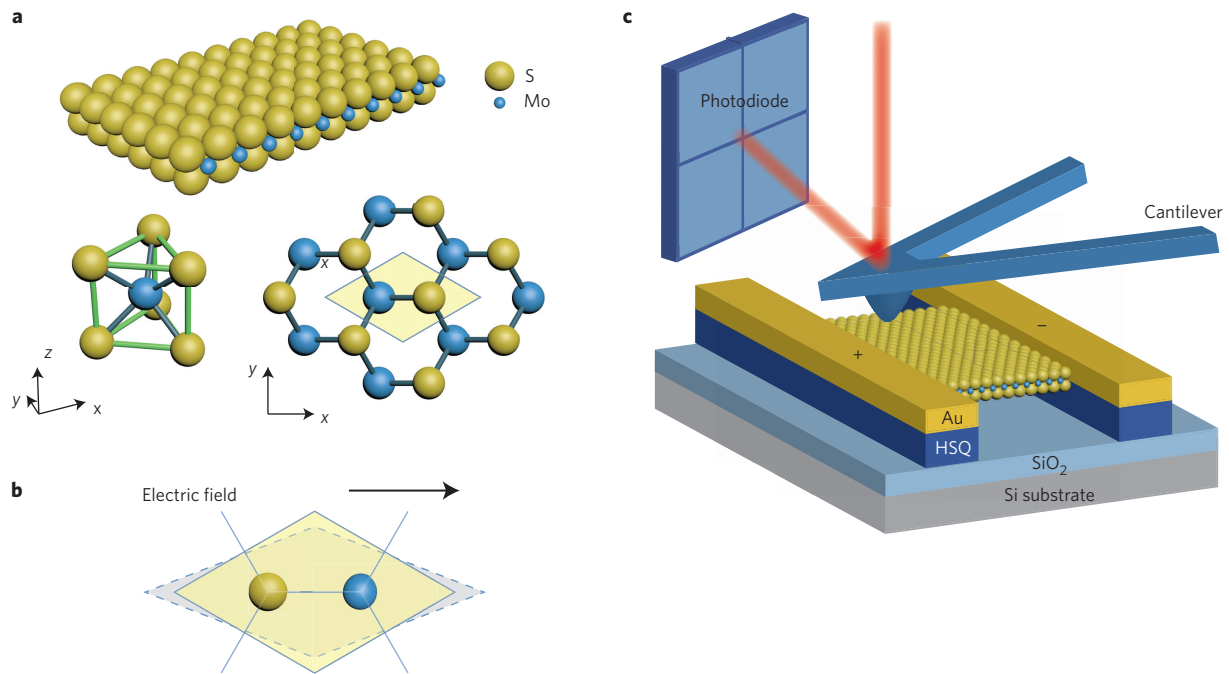


Figure 1 | Probing the piezoelectric property of free-standing monolayer MoS₂. **a**, A single layer of MoS₂ consists of S-Mo-S stacking with a total thickness of 0.6 nm, with the Mo atom centred in the trigonal prism (bottom left). Viewing from the top (bottom right), each unit cell (denoted by the yellow shadow) consists of two S atoms occupying the same site in the hexagonal lattice, with the Mo atom residing in the opposite site, therefore breaking inversion symmetry in the *x*-*y* plane but preserving mirror symmetry in the *z* direction (Supplementary Fig. 1). **b**, With an external electric field pointing from the S site to the Mo site, the Mo-2S dipole is stretched and the unit cell is elongated, creating compressive stress in the *x* direction and tensile stress in the *y* direction. **c**, To measure the in-plane piezoelectric stress, the MoS₂ film was suspended on two HSQ posts, clamped underneath by two Au electrodes. The film was indented with a scanning AFM probe. The induced stress changed the load on the cantilever, which was observed by the deflection of a laser beam.

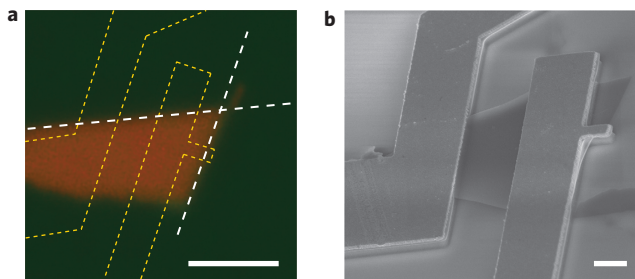


Figure 2 | Design and characterization of the piezoelectric monolayer MoS₂ device. **a**, To maximize piezoelectric coupling, electrodes (outlined with yellow dashed lines) were defined parallel to the zigzag edges (white dashed lines, verified by SHG measurements) of the exfoliated monolayer flakes, identified by confocal fluorescence microscopy. The false colours of green and red denote the intensity of reflection and photoluminescence, respectively. Scale bar, 5 μm . **b**, The device was inspected by SEM to confirm that free-standing MoS₂ monolayers were clamped between the Au electrodes and HSQ posts, patterned via one-step EBL. The clearance between film and substrate was large enough (>450 nm) to reduce the van der Waals force from the substrate during indentation. Scale bar, 1 μm .

The free-standing single-layer MoS₂ devices were fabricated from exfoliated monolayer flakes on poly-methyl-methacrylate (PMMA). The flakes and the PMMA layer were transferred together onto hydrogen silsesquioxane (HSQ), and the monolayers of MoS₂ between the PMMA/HSQ layers were identified by confocal fluorescence microscopy (Fig. 2a, Supplementary Fig. 2). To apply an electric field along the armchair direction, the electrodes were designed to be parallel to or at 60° with respect to the sharply cleaved edges which form 60° or 120° corners. The direction was confirmed by SHG (Supplementary Figs 3 and 4)^{18,19}. Suspension,

mechanical clamping and electrical contact were simultaneously achieved in the areas enclosed by yellow dashed lines in Fig. 2a by one-step electron-beam lithography (EBL). Crosslinked HSQ (amorphous SiO₂) formed supporting posts under the MoS₂ membrane, and the PMMA was removed to open a window for Au electrodes on top (Fig. 2b, Supplementary Fig. 5). After inspecting the membrane by AFM in non-contact mode, we measured the load and piezoelectric response as a function of depth through indentation in contact mode. A large-radius tip was used to minimize peak stress in the film and to avoid potential damage (Supplementary Fig. 6).

The load-indentation relation of a clamped membrane (used to determine the material properties) was deduced by means of finite element calculations. The width of the membrane was set to be much larger than its length between clamps, so that the load was insensitive to variations in the shape and distance between free edges. Within the regime of small indentation, the elastic response of the membrane without electric field was determined by its Young's modulus Y^{2D} , Poisson's ratio ν and pre-stress σ^{2D} in cubic polynomial form with two geometry-dependent pre-factors²⁷. Taking $\nu = 0.25$ from ref. 7, we found the load of the membrane could be described by

$$F = 2.1\sigma^{2D}L(d/L) + 3.1Y^{2D}L(d/L)^3 \quad (2)$$

where L is the distance between the electrodes and d is the depth of indentation (Supplementary Fig. 7). Figure 3a shows the fitting of experimental data on a monolayer MoS₂ device with $Y^{2D} = (1.2 \pm 0.1) \times 10^2 \text{ N m}^{-1}$ and $\sigma^{2D} = 45 \pm 5 \text{ mN m}^{-1}$, which agrees well with previous *ab initio* calculations and experimental results^{7,28}. The repeatable load-indentation curves demonstrated the quality of the atomic crystalline film and the effectiveness of the clamp.

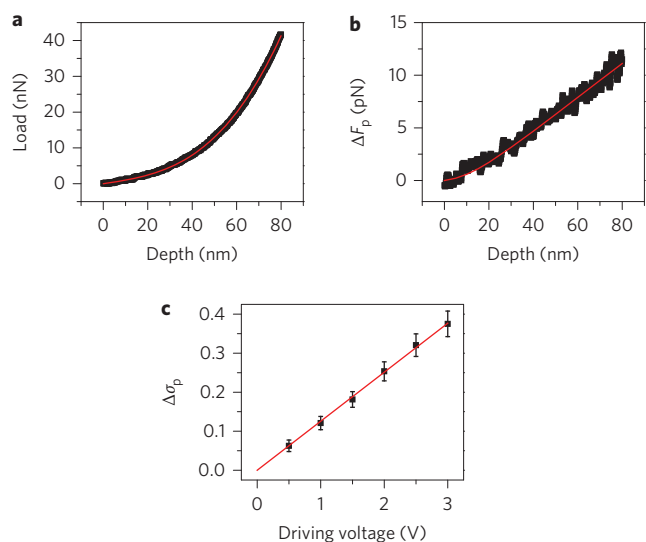


Figure 3 | Measuring the piezoelectric coefficient through nano-indentation and electromechanical actuation. **a**, The mechanical properties of MoS₂ membranes without an electric field are characterized by the load-indentation dependence (black scatter). The vertical load exhibits a cubic dependence on indentation depth described by linear elastic membrane theory (equation (2)). The Young's modulus ($\gamma^{2D} = 1.2 \times 10^2 \text{ N m}^{-1}$) of monolayer MoS₂ retrieved from a polynomial fitting curve (red) was in good agreement with previous studies. The load curve also provides an effective spring constant of the film as a function of depth. **b**, Piezoelectrically induced load (ΔF_p) on the tip at fixed driving voltage ($V = 1 \text{ V}$) measured as a function of depth of indentation (black scatter). The slope of the fitting curve (red) is the scalar piezoelectric stress ($\Delta\sigma_p = 0.12 \text{ mN m}^{-1}$) according to equation (3). ΔF_p was derived from the stiffness of the tip/film assembly multiplied by the change of tip deflection Δz directly measured with a lock-in amplifier. **c**, Piezoelectric stress measured at various driving voltage (black scatter) at a fixed depth of indentation shows a linear dependence. The error bars (standard uncertainty) are estimated from the noise level. The piezoelectric coefficient of monolayer $e_{11} = 2.9 \times 10^{-10} \text{ C m}^{-1}$ was calculated from the slope of the fitting curve (red).

With the electric field, the induced piezoelectric stress $\Delta\sigma_p$ in MoS₂ was treated as a perturbation during indentation, because it was two orders of magnitude smaller than the pre-stress σ^{2D} of the suspended film, according to our experimental conditions and the theoretical value of the electromechanical coupling strength. This stress provided an additional piezoelectric load ΔF_p to the film under indentation, which can be approximated as

$$\Delta F_p = 1.3(\Delta\sigma_p)d \quad (3)$$

This additional load was measured by the tip displacement Δz via $\Delta F_p = (k_t + k_m)\Delta z$, where k_t is the stiffness of the AFM cantilever and $k_m = \partial F/\partial d$ is the stiffness of the MoS₂ membrane derived from the load-indentation relation (equation (2)). The numerical pre-factor 1.3 is smaller than the one preceding σ^{2D} (2.1) in equation (2) as a result of the anisotropic piezoelectric stress.

Due to the small force (ΔF_p on the scale of $\sim \text{pN}$) and displacement (Δz on the scale of $\sim \text{pm}$) involved, a phase lock-in scheme was used where $\Delta\sigma_p$ was modulated by an alternating electric field and Δz was measured at the same frequency. The frequency of electrical actuation ($f_p \approx 10 \text{ kHz}$) was kept well below the fundamental resonance of the tip-film system ($f_0 \approx 100 \text{ kHz}$) so that the previous quasi-stationary mechanical model was applicable. The lock-in amplification effectively rejected higher-order non-piezoelectric effects that are proportional to the square of the applied voltage,

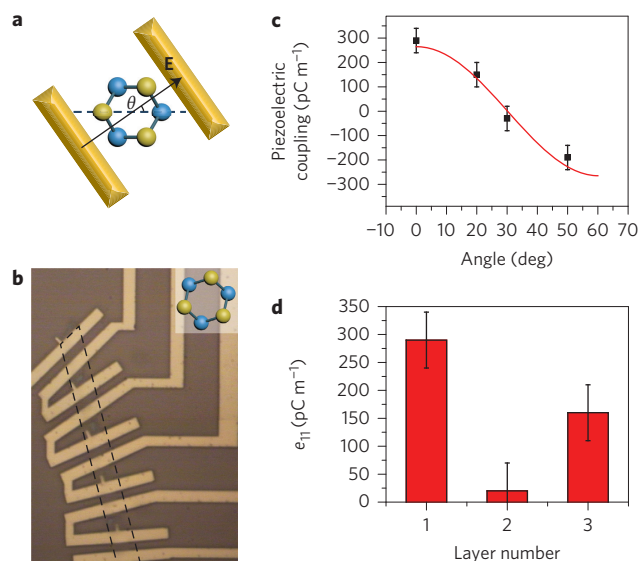


Figure 4 | Angular dependence of the piezoelectric response in monolayer MoS₂. **a**, The rotation of the crystal with respect to the electric field and mechanical boundary was achieved by patterning the electrodes at different angles θ . **b**, Optical image of multiple electrode pairs integrated on a long stripe of MoS₂ (dashed outline) rotated by 10° at each section. The relative rotation between the first and last device is 60° , so the piezoelectric effect should reverse sign as the alignment of the electric field to the Mo-2S dipole changes from parallel to antiparallel. Scale bar, $10 \mu\text{m}$. **c**, Measured piezoelectric coupling strength (square data points) followed the $\cos 3\theta$ dependence (the red fitting curve) predicted from the crystalline three-fold symmetry. The sign change was observed from the phase readout of the piezoelectric signal through a lock-in amplifier. This distinguished our low-frequency electric method from SHG (which typically only gives amplitude information), enabling the crystalline orientation (as shown in the inset of **b**) to be uniquely determined without resorting to atomic images. **d**, Measured piezoelectric coefficient in one-, two- and three-layer MoS₂ membranes, showing that only odd numbers of layers exhibit a significant coupling strength due to their broken inversion symmetry. Error bars (standard uncertainty) in **c** and **d** were estimated from the noise level of the force measurement and variations in the device geometry.

such as thermal expansion by Joule heating, the capacitive pressure between film and substrate and electrostriction. To eliminate the oscillating spurious force at the same frequency as the driving voltage from the static charge or contact potential difference between surfaces, we used a conductive tip and a degenerately doped silicon substrate²⁴. Both were biased with respect to the membrane to balance the contact potential until the electrostatic force was minimized (Supplementary Methods)²⁹.

As shown in Fig. 3b, we observed a linear dependence of piezoelectric load ΔF_p on indentation depth, in agreement with equation (3). The load curve approaches the origin at zero indentation depth, which clearly verifies the absence of electrostatic force. At a fixed driving voltage ($V = 1 \text{ V}$), fitting of the depth dependence of ΔF_p with the finite element calculation (red curve) resulted in a piezoelectric stress of $\Delta\sigma_p = 0.12 \pm 0.02 \text{ mN m}^{-1}$. A positive sign was assigned because the signal and the driving voltage were in phase. Meanwhile, the piezoelectric stress at a fixed depth of indentation increased with ramping driving voltage (Fig. 3c), with a linear fit according to equation (1) giving $e_{11} = (2.9 \pm 0.5) \times 10^{-10} \text{ C m}^{-1}$ (or

0.5 C m^{-2} when normalized by the layer thickness), close to a reported result calculated by density functional theory⁷. The measured piezoelectric coefficient is comparable to the bulk values of standard piezoelectric crystals such as ZnO or AlN.

The MoS₂ monolayer experiences a tensile strain when a positive voltage drop is applied. Because the sign of e_{11} is positive according to theory⁹, the electric field is along the Mo → S bond direction (equation (1)). Accordingly, the anisotropy of piezoelectricity in monolayer MoS₂ offers a mesoscopic way (under ambient conditions) to unambiguously determine its crystalline orientation by distinguishing a crystal from its inverse structure. Previously, this was only achieved in ultrahigh-vacuum (UHV) environment using atomic imaging tools^{30,31}. Due to the symmetry of the D_{3h} group, the piezoelectric coupling of the MoS₂ monolayer is a function of the crystal's azimuthal angle θ between the mirror plane containing the axis of rotation in the crystal structure and the direction of the electric field (Fig. 4a):

$$\Delta\sigma_p/E = -e_{11} \cos 3\theta \quad (4)$$

Although the shear force term $\Delta\sigma_{12}$ becomes non-zero when $\theta \neq 0$, it makes no contribution to the load of the tip (Supplementary Fig. 8). Hence, we can still extract the piezoelectric stress using equation (3). We fabricated a series of devices based on the same single-crystal flake to study the angular dependence (Fig. 4b), with θ ranging from 0° to 60° . The piezoelectric coupling of these devices (Fig. 4c) fit well to a cosine curve (red solid line) with a period of 120° and an angular error of less than 2° , in accordance with the crystalline orientation inferred from SHG. The change of sign from the upper devices to the lower ones allowed us to assign the atomic orientation to the two-dimensional crystal as overlaid in the optical image.

We also studied the thickness dependence of the piezoelectric coefficient of two-dimensional membranes exfoliated from natural 2H-MoS₂ crystals. We observed a piezoelectric response only for odd-layer membranes due to inversion symmetry breaking (Fig. 4d). For even-layer membranes, the contributions to piezoelectricity from alternating orientations of adjacent layers cancelled. Such results in two-dimensional crystals mark the distinctive thickness dependence of the piezoelectric coefficient from the linear scaling of conventional piezoelectric materials. The strain-gradient-induced piezoelectric coupling or 'flexoelectricity' was estimated to generate ~ 0.1 pN force, more than one order of magnitude lower than the force from piezoelectricity³², as the curvature of the indented membrane in our experiment was small. Common sources of error for AFM measurements such as the hysteresis of the piezo tube and tip degradation were constantly monitored. The angular and layer dependence of the electromechanical response of the devices also provided independent evidence that the signal in our measurement originated from the piezoelectricity of MoS₂.

In conclusion, we have reported the observation of molecular piezoelectricity in free-standing monolayer MoS₂ crystals. In contrast to bulk piezoelectric materials, we show that such two-dimensional piezoelectricity only exists when there are an odd number of layers due to inversion symmetry breaking. We found that the angular dependence of piezoelectricity provides a mesoscopic method to probe the absolute orientation of two-dimensional crystals, which is crucial for valleytronic devices and edge engineering. As flexural rigidity scales inversely with device thickness, two-dimensional piezoelectric materials could greatly enhance mechanical displacement and therefore sensitivity. The robust piezoelectricity of such materials makes them excellent material choices for atomically thin piezoelectric devices³³. With their reduction in size, weight and energy consumption, such two-dimensional piezoelectric materials will make profound impacts in

ultrasensitive sensors, nanoscale electromechanical systems and the next generation of low-power electronics.

Note added in proof: While this manuscript was under review, an independent study on a similar topic (ref. 22) was published.

Methods

Sample fabrication. Atomically thin crystals of MoS₂ were exfoliated on a PMMA/aquaSAVE (water-soluble polymer) stack. The PMMA layer was released in water and transferred onto HSQ. The thickness and uniformity of the MoS₂ was characterized by scanning photoluminescence (Nikon TE-2000, excitation wavelength of 488 nm and collected with a 650 nm longpass filter) and Raman spectrum (Horiba, excitation wavelength of 473 nm) measurements. After EBL and metal deposition, the film was released via critical point drying. Scanning electron microscopy (SEM) images were recorded with an LEO 1550 microscope.

Electrical measurement. During piezoelectric measurements, the voltage across the MoS₂ film was applied by a delay generator (Stanford Research DG535) that provided two out-of-phase square waves with tunable amplitude and d.c. offset to the opposite electrodes of the device, providing an oscillating electric field while maintaining a constant electric potential in the centre of the film. The oscillation of the cantilever was read by a lock-in amplifier (Stanford Research 830) through a signal access module (Digital Instrument). Details can be found in the Supplementary Methods.

Received 26 September 2014; accepted 21 November 2014;
published online 22 December 2014

References

- Shirane, G., Hoshino, S. & Suzuki, K. X-ray study of the phase transition in lead titanate. *Phys. Rev.* **80**, 1105–1106 (1950).
- Bernardini, F., Fiorentini, V. & Vanderbilt, D. Spontaneous polarization and piezoelectric constants of III–V nitrides. *Phys. Rev. B* **56**, 10024–10027 (1997).
- Zhang, Q. M., Bharti, V. & Zhao, X. Giant electrostriction and relaxor ferroelectric behavior in electron-irradiated poly(vinylidene fluoride-trifluoroethylene) copolymer. *Science* **280**, 2101–2104 (1998).
- Xiang, H. J., Yang, J., Hou, J. G. & Zhu, Q. Piezoelectricity in ZnO nanowires: a first-principles study. *Appl. Phys. Lett.* **89**, 223111 (2006).
- Li, S. P. *et al.* Size effects in nanostructured ferroelectrics. *Phys. Lett. A* **212**, 341–346 (1996).
- Novoselov, K. S. *et al.* Two-dimensional atomic crystals. *Proc. Natl Acad. Sci. USA* **102**, 10451–10453 (2005).
- Duerloo, K.-A. N., Ong, M. T. & Reed, E. J. Intrinsic piezoelectricity in two-dimensional materials. *J. Phys. Chem. Lett.* **3**, 2871–2876 (2012).
- Marx, K. A. Quartz crystal microbalance: a useful tool for studying thin polymer films and complex biomolecular systems at the solution-surface interface. *Biomacromolecules* **4**, 1099–1120 (2003).
- Masmanidis, S. C. *et al.* Multifunctional nanomechanical systems via tunably coupled piezoelectric actuation. *Science* **317**, 780–783 (2007).
- Luo, Y. *et al.* Nanoshell tubes of ferroelectric lead zirconate titanate and barium titanate. *Appl. Phys. Lett.* **83**, 440–442 (2003).
- Wang, Z. L. & Song, J. H. Piezoelectric nanogenerators based on zinc oxide nanowire arrays. *Science* **312**, 242–246 (2006).
- Nguyen, T. D. *et al.* Piezoelectric nanoribbons for monitoring cellular deformations. *Nature Nanotech.* **7**, 587–593 (2012).
- Sai, N. & Mele, E. J. Microscopic theory for nanotube piezoelectricity. *Phys. Rev. B* **68**, 241405 (2003).
- Quan, X., Marvin, C. W., Seebald, L. & Hutchison, G. R. Single-molecule piezoelectric deformation: rational design from first-principles calculations. *J. Phys. Chem. C* **117**, 16783–16790 (2013).
- Mak, K. F., He, K., Shan, J. & Heinz, T. F. Control of valley polarization in monolayer MoS₂ by optical helicity. *Nature Nanotech.* **7**, 494–498 (2012).
- Cao, T. *et al.* Valley-selective circular dichroism of monolayer molybdenum disulphide. *Nature Commun.* **3**, 887 (2012).
- Zeng, H., Dai, J., Yao, W., Xiao, D. & Cui, X. Valley polarization in MoS₂ monolayers by optical pumping. *Nature Nanotech.* **7**, 490–493 (2012).
- Li, Y. *et al.* Probing symmetry properties of few-layer MoS₂ and h-BN by optical second-harmonic generation. *Nano Lett.* **13**, 3329–3333 (2013).
- Yin, X. *et al.* Edge nonlinear optics on a MoS₂ atomic monolayer. *Science* **344**, 488–490 (2014).
- Nye, J. F. *Physical Properties of Crystals: Their Representation by Tensors and Matrices* (Reproduced with corrections and new material, 1985) (Clarendon, 1957).
- Wang, Z., Hu, J., Suryavanshi, A. P., Yum, K. & Yu, M.-F. Voltage generation from individual BaTiO₃ nanowires under periodic tensile mechanical load. *Nano Lett.* **7**, 2966–2969 (2007).
- Wu, W. *et al.* Piezoelectricity of single-atomic-layer MoS₂ for energy conversion and piezotronics. *Nature* **514**, 470–474 (2014).

23. Gruverman, A., Auciello, O. & Tokumoto, H. Nanoscale investigation of fatigue effects in Pb(Zr,Ti)O₃ films. *Appl. Phys. Lett.* **69**, 3191–3193 (1996).
24. Christman, J. A., Woolcott, R. R., Kingon, A. I. & Nemanich, R. J. Piezoelectric measurements with atomic force microscopy. *Appl. Phys. Lett.* **73**, 3851–3853 (1998).
25. Minary-Jolandan, M., Bernal, R. A., Kujanishvili, I., Parpoil, V. & Espinosa, H. D. Individual GaN nanowires exhibit strong piezoelectricity in 3D. *Nano Lett.* **12**, 970–976 (2012).
26. Lee, C., Wei, X., Kysar, J. W. & Hone, J. Measurement of the elastic properties and intrinsic strength of monolayer graphene. *Science* **321**, 385–388 (2008).
27. Pan, J. Y., Lin, P., Maseeh, F. & Senturia, S. D. Verification of FEM analysis of load-deflection methods for measuring mechanical properties of thin films. *Technical Digest IEEE Solid-State Sensor and Actuator Workshop* (cat. no. 90CH2783-9), 70–73 (1990).
28. Bertolazzi, S., Brivio, J. & Kis, A. Stretching and breaking of ultrathin MoS₂. *ACS Nano* **5**, 9703–9709 (2011).
29. Kalinin, S. V. *et al.* Nanoscale electromechanics of ferroelectric and biological systems: a new dimension in scanning probe microscopy. *Annu. Rev. Mater. Res.* **37**, 189–238 (2007).
30. Helveg, S. *et al.* Atomic-scale structure of single-layer MoS₂ nanoclusters. *Phys. Rev. Lett.* **84**, 951–954 (2000).
31. Van der Zande, A. M. *et al.* Grains and grain boundaries in highly crystalline monolayer molybdenum disulfide. *Nature Mater.* **12**, 554–561 (2013).
32. Naumov, I., Bratkovsky, A. M. & Ranjan, V. Unusual flexoelectric effect in two-dimensional noncentrosymmetric *sp*²-bonded crystals. *Phys. Rev. Lett.* **102**, 217601 (2009).
33. Lopez-Suarez, M., Pruneda, M., Abadal, G. & Rurall, R. Piezoelectric monolayers as nonlinear energy harvesters. *Nanotechnology* **25**, 175401 (2014).

Acknowledgements

This work was supported by the US Department of Energy, Basic Energy Sciences Energy Frontier Research Center (DoE-LMI-EFRC) under award DOE DE-AC02-05CH11231.

Author contributions

X.Z., X.Y., H.Z. and Z.J.W. conceived the project. H.Z., M.L. and Y.Y. developed the sample design and fabricated the samples. H.Z. and Y.W. performed the measurements. H.Z., S.X. and Z.J.W. carried out the mechanical analysis. J.X., H.Z. and Z.Y. performed the optical measurements. H.Z. and Z.Y. conducted electrical analysis. All authors contributed to writing the manuscript.

Additional information

Supplementary information is available in the [online version](#) of the paper. Reprints and permissions information is available online at www.nature.com/reprints. Correspondence and requests for materials should be addressed to X.Z.

Competing financial interests

The authors declare no competing financial interests.